Supplementary Data:

Investigating the human Calcineurin Interaction Network using the πϕLxVP SLiM

Sarah R. Sheftic[1], Rebecca Page[2] and Wolfgang Peti[1,3*]

Table S1. Abbreviations.

Abbreviations	
Ca^{2+}	calcium ion
IDP	intrinsically disordered protein
IDR	intrinsically disordered region
ITC	Isothermal titration calorimetry
IUPRED	Programs used to predict of the structural propensity of proteins
PSP	protein ser/thr phosphatase
SLiM	short linear motif
SLiM sequences	
LxVP	SLiM also specific for CN (L, leucine; V, valine)
ϕLxVP	SLiM in which ϕ represents a hydrophobic amino acid
πϕLxVP	SLiM in which π represents a polar amino acid
PxIxIT	SLiM specific for CN (P, proline; x, any amino acid, I, isoleucine; T, threonine)
WxF	sequence motif just C-terminal to the LxVP sequence in NFATs
Gene/proteins	
AKAPs	A-kinase anchor proteins
BRAC1/BRAC2	breast cancer 1 or 2 protein
CBLB	Cbl Proto-Oncogene B
CN	calcineurin
CNA	the A-subunit of calcineurin
CNB	the B-subunit of calcineurin
Cux1	Cut Like Homeobox 1
DNML1	dynamin 1 like protein; a CN substrate
ELK	transcription factor
EMSY	BRAC2 interacting transcriptional repressor
HER2C	HECT And RLD Domain Containing E3 Ubiquitin Protein Ligase 2
JNK	c-jun N-terminal kinase
MAP3K	Mitogen activate protein kinase kinase kinase
MED	Mediator Complex Subunit
MSL1	Male Specific Lethal 1 Homolog
NFAT/NFATc1-c4	nuclear factor of activated T-cells c1-c4
PALB2	partner and localizer of BRAC2
PCD1/PCD2	positively charged domains 1 and 2
PKA subunit RII	cAMP-Dependent Protein Kinase A regulatory subunit-II A
PKC	Protein kinase C

SIX4	Sine Oculis Homeobox Homolog 4
SYDE2	Synapse Defective Protein 1 Homolog 2
TP53BP1	Tumor suppressor p53-binding protein 1

Table S2. Data collection and refinement statistics

	CNA$_{1-370}$,CNB$_{1-169}$; NFAT LxVP peptide[a]
Data collection	
Space group	P 2_1 2_1 2_1
Cell dimensions	
a, b, c (Å)	57.7, 106.0, 111.9
α, β, γ (°)	90, 90, 90
Resolution (Å)	39.04 - 2.60 (2.71 - 2.60) *
R_{merge}	0.115 (0.805)
Mean $I / \sigma I$	4.7 (1.7)
Completeness (%)	99.6 (97.8)
Redundancy	7.3 (7.2)
CC$_{1/2}$	0.998 (0.773)
Refinement	
Resolution (Å)	39.03 – 2.60
No. reflections	21785
R_{work} / R_{free}	0.19/0.24
No. atoms	
Protein	4333
Ligand/ion	58
Water	52
B-factors	
Protein	47.40
Ligand/ion	53.30
Water	41.60
R.M.S. deviations	
Bond lengths (Å)	0.004
Bond angles (°)	0.597
Ramachandran	
Outliers (%)	0.00
Allowed (%)	4.4
Favored (%)	95.6

[a]Data was collected from a single crystal
*Values in parentheses are for highest-resolution shell.

Table S3: ITC data

CN	NFAT Peptides	K_D (μM)	ΔH (kcal*Mol^{-1})	TΔS (kcal*Mol^{-1})
(A) 1-370 (B) 1-169	[383]DDQYL<u>AVP</u>QHPYQWAKPK[400]	1.8 ± 0.1	-19.5 ± 0.2	-11.7 ± 2.2
(A) 1-370 (B) 1-169	[383]DDQYL<u>AVP</u>QH[392]	1.6 ± 0.3	-3.1 ± 0.9	4.8 ± 0.8
(A) 1-348	[116]ESPRIEITS[124]	4.1 ± 0.1	-1.5 ± 0.2	5.8 ± 0.2
(A) 1-348	[383]DDQYL<u>AVP</u>QHPYQWAKPK[400]	2.4 ± 0.2	-1.1 ± 0.1	-6.5 ± 0.1
(A) 1-348	[383]DDQYL<u>AVP</u>QH[392]	No binding	n/a	n/a
	New Substrates			
(A) 1-370 (B) 1-169	[178]PALB2[275]	3.1 ± 1.6	-2.6 ± 1.4	5.0 ± 1.2
(A) 1-370 (B) 1-169	[232]SYDE2[289]*	2.6 ± 0.08	-3.2 ± 1.8	4.5 ± 1.8

Average of ≥3 ITC experiments for all data points.
*Average of 2 ITC experiments.

Table S4. Proteins in CN^{CON}

	Uniprot ID	Protein		Uniprot ID	Protein
1	P49418	AMPH	25	P11137	MAP2
2	Q92934	BAD	26	P10636	MAPT
3	P15056	BRAF (RAF)	27	Q9NP98	MYOZ1
4	Q13936	CACNA1C	28	Q9NPC6	MYOZ2
5	P27824	CANX	29	Q8TDC0	MYOZ3
6	Q9Y2V2	CARHSP1	30	P12036	NEFH
7	O95180	CAC1H	31	O95644	NFATC1
8	P02489	CRYAA	32	Q13469	NFATC2
9	P49674	CSNK1E (CK1)	33	Q12968	NFATC3
10	Q05193	DNM1	34	Q14934	NFATC4
11	O00429	DNM1L	35	Q08499	PDE4D
12	P50570	DNM2	36	Q13522	PPP1R1A
13	P11532	DMD	37	Q9UD71	PPP1R1B
14	P19419	ELK1	38	P13861	PRKAR2A
15	Q9Y6I3	EPN1	39	P06400	RB1
16	P42566	EPS15	40	P53805	RCAN1
17	P21333	FLNA	41	Q14206	RCAN2
18	P42261	GRIA1	42	Q9UKA8	RCAN3
19	P49841	GSK3B (GSK)	43	P19634	SL9A1
20	P56537	IF6	44	O60641	SNAP91, AP180
21	P05412	JUN	45	Q8WYL5	SSH1
22	P13861	KAP2	46	O43426	SYNJ1
23	Q7Z418	KCNK18	47	Q5T7P8	SYT6
24	Q6VAB6	KSR2	48	P31629	Zep2

Figure S1.

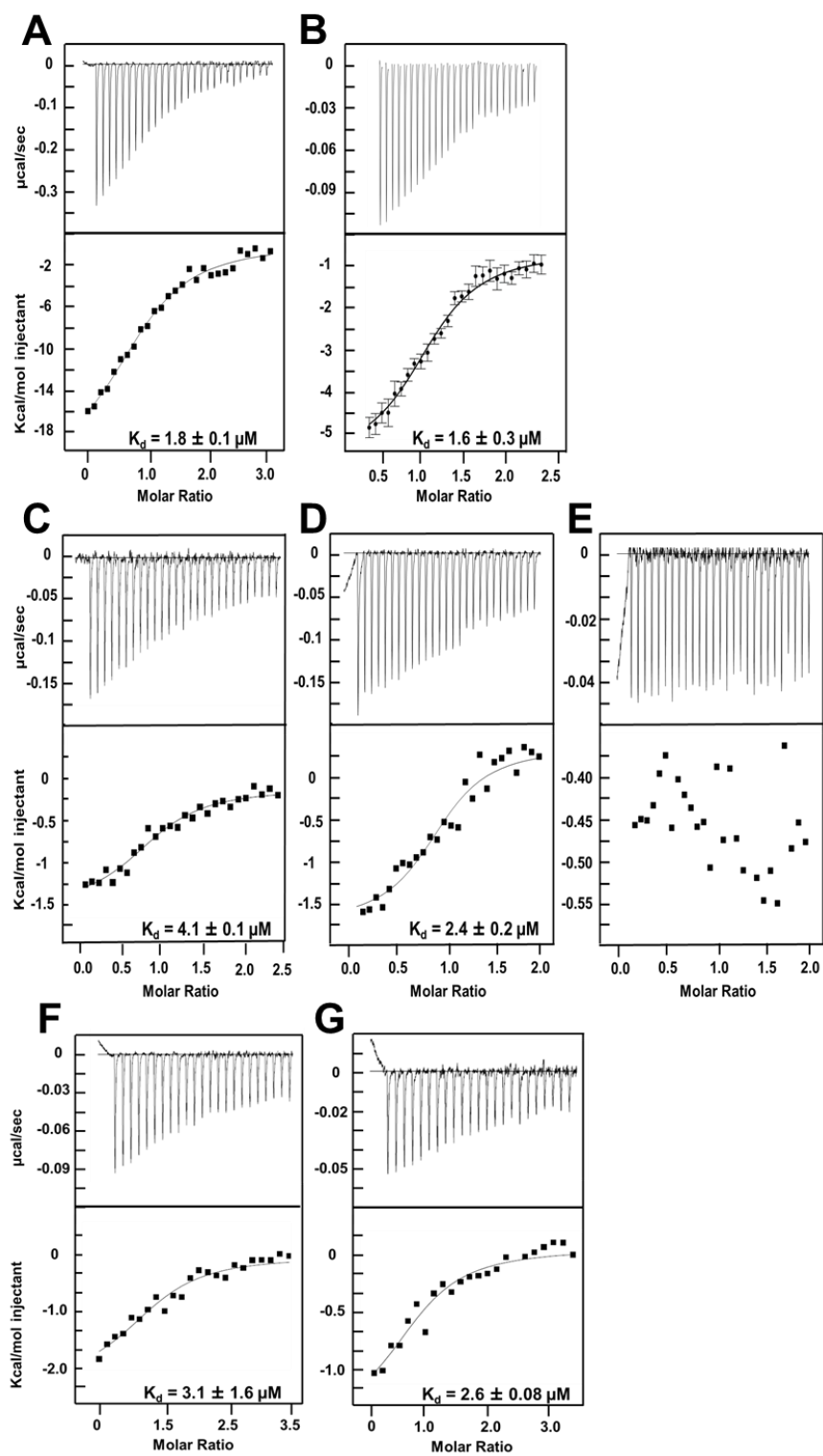**Figure S1.** *NFATc1 binds to CN via a short πϕLxVP motif and requires CNA and CNB.* Isothermal titration calorimetry (ITC) data for CN (A: 1-370, B: 1-169) with NFATc1 substrates **(A)** LxVP$_{long}$ peptide: ^{383}DDQY<u>LAVP</u>QHPYQ<u>WAK</u>PK^{400} and **(B)** LxVP$_{short}$ peptide: ^{383}DDQY<u>LAVP</u>QH^{392}. ITC data for CNA (1-348) with NFATc1 **(C)** PxIxIT peptide ^{116}ES<u>PRIEITS</u>^{124} **(D)** LxVP$_{long}$ peptide: ^{383}DDQY<u>LAVP</u>QHPYQ<u>WAK</u>PK^{400} and **(E)** LxVP$_{short}$ peptide: ^{383}DDQY<u>LAVP</u>QH^{392}. ITC data for CN (A: 1-370, B: 1-169) with substrates **(F)** PALB2 protein (residues 178-275) and **(G)** SYDE2 protein (residues 232-289). Raw thermograms and the corresponding curve fits with a stoichiometry n=1 are shown. Thermodynamic parameters are listed in **Table S1**.
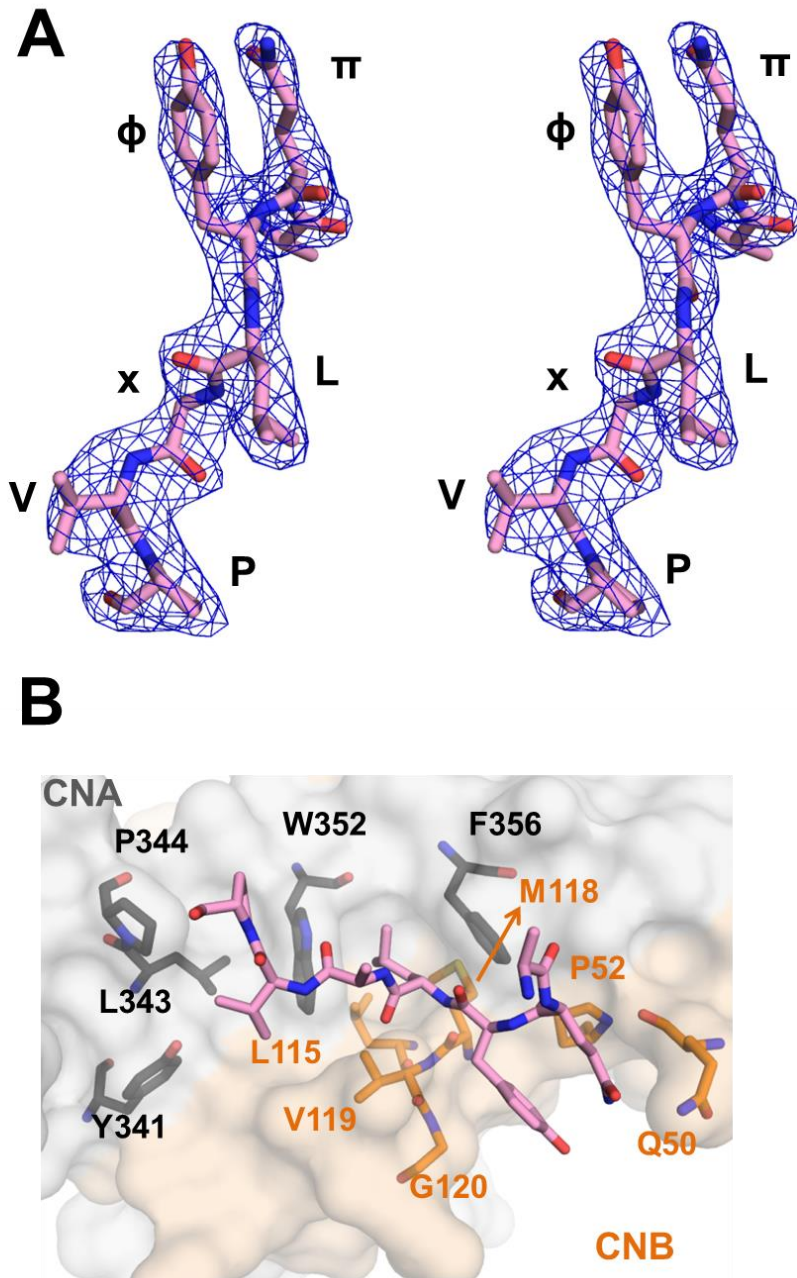
Figure S2.

Figure S2. *NFATc1 πϕLxVP binding is mainly driven by hydrophobic, but also a few critical electrostatic interactions*. **A)** Stereo-view of the NFATc1 LxVP motif. Electron density of the NFATc1 LxVP peptide visible residues ([384]DQYLAVP[390]) shown as blue mesh (2F$_o$-F$_c$, σ = 1.0). **B)** Residues of CNA (dark grey sticks) and CNB (orange sticks) that mediate hydrophobic contacts with NFATc1 LxVP are shown.
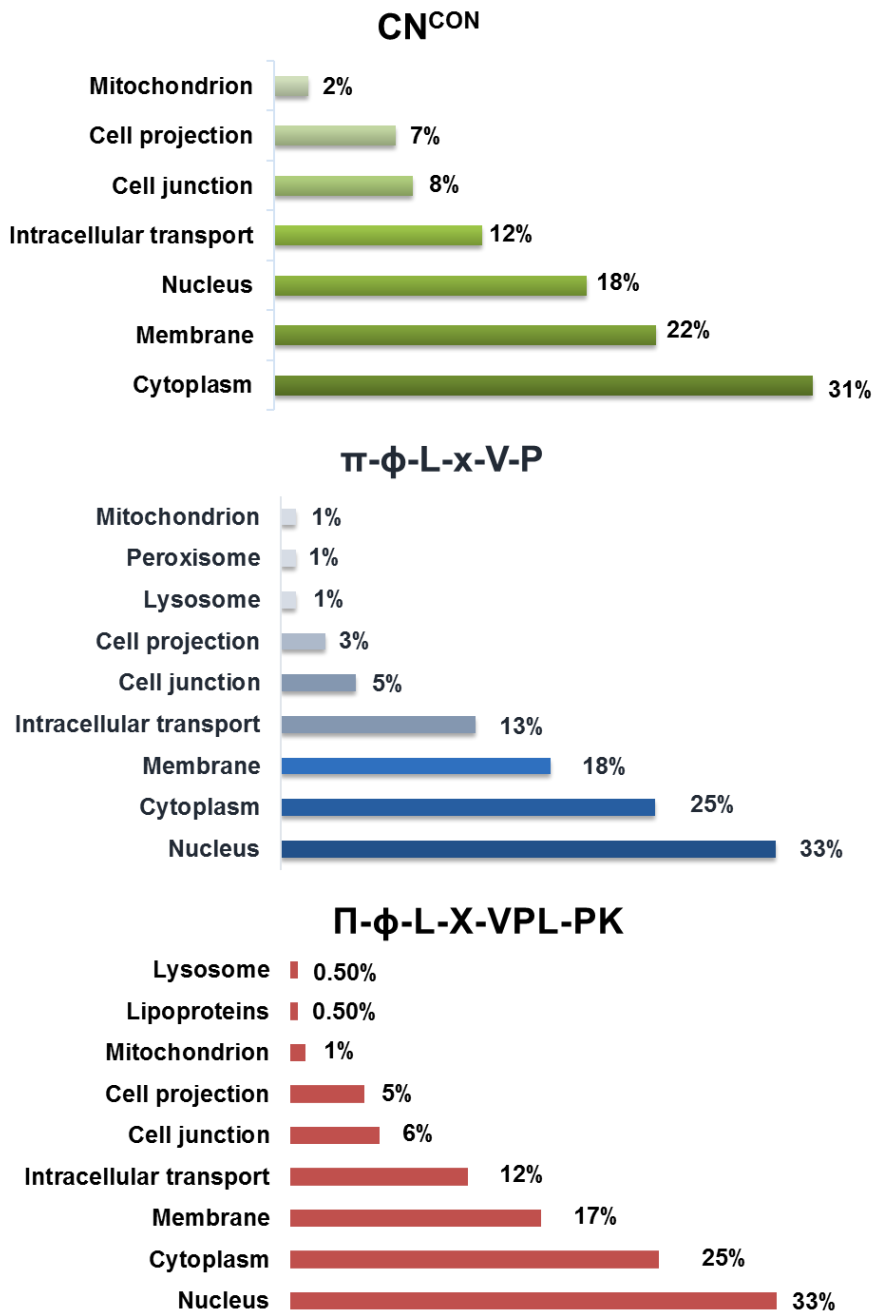
Figure S3.

Figure S3. *The cellular distribution of CN substrates remains highly similar among all 3 databases*. Cellular distribution of the 48 proteins represented in CN^CON (green), the 91 proteins that contain putative π-ɸ-L-x-**V-P** motifs (blue) and the 565 proteins that contain putative π-ɸ-L-x-**VPL-PK** motifs (red). Proteins from the π-ɸ-L-x-**V-P** and π-ɸ-L-x-**VPL-PK** databases also contain putative PxIxIT SLiMs contained in IDRs and experimentally confirmed pSer/pThr residues (UniProt).
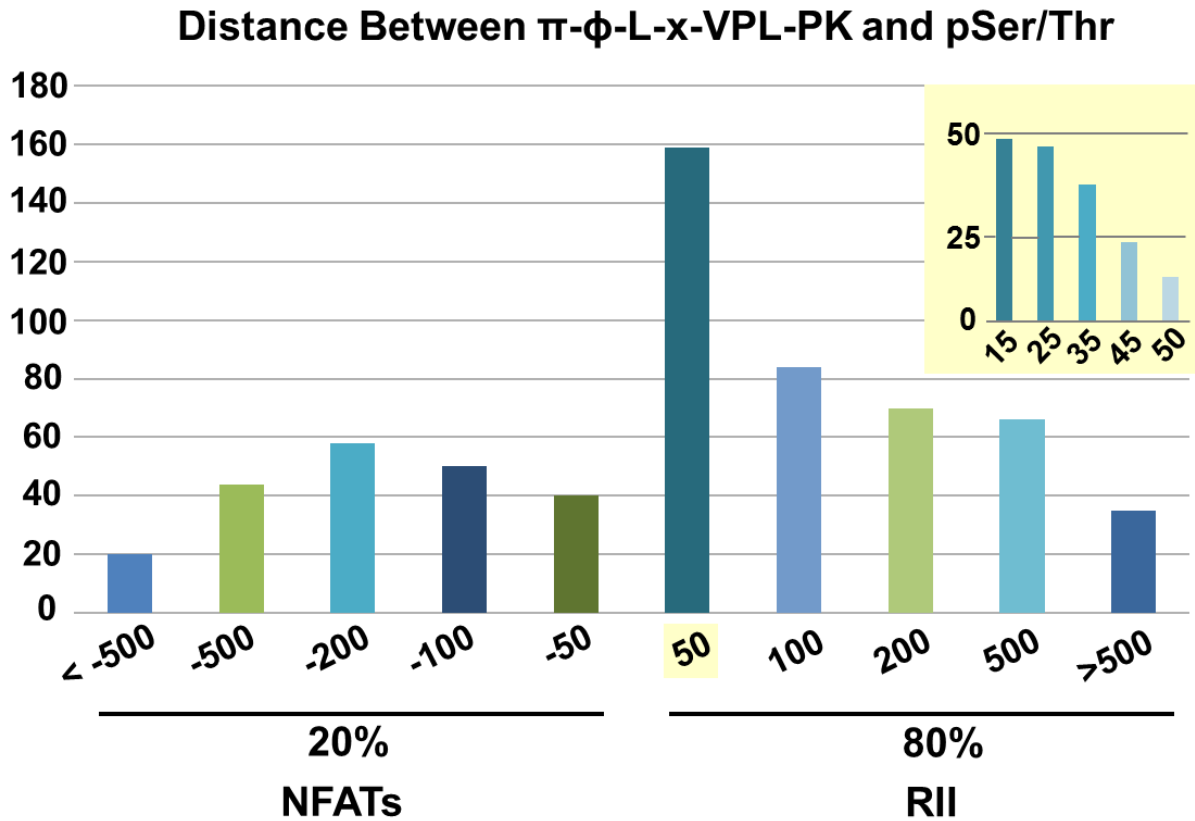
Figure S4.

Figure S4. *Distribution of phosphosite distances from the π-ɸ-L-x-VPL-PK SLiM.* Distances (number of residues) between the nearest pSer/Thr residue from the predicted π-ɸ-L-x-VPL-PK SLiM of the interacting proteins. Phosphosites N- and C-terminal to the SLiM were considered. A minimum distance of 9 residues for C-terminal and 20 residues for N-terminal pSer/pThr sites were used as cutoffs based on the distance between the active site and the π-ɸ-L-x-VPL-PK SLiM binding site. For interacting proteins with multiple predicted π-ɸ-L-x-VPL-PK SLiMs, the pSer/pThr residues nearest to each motif were used for this analysis.
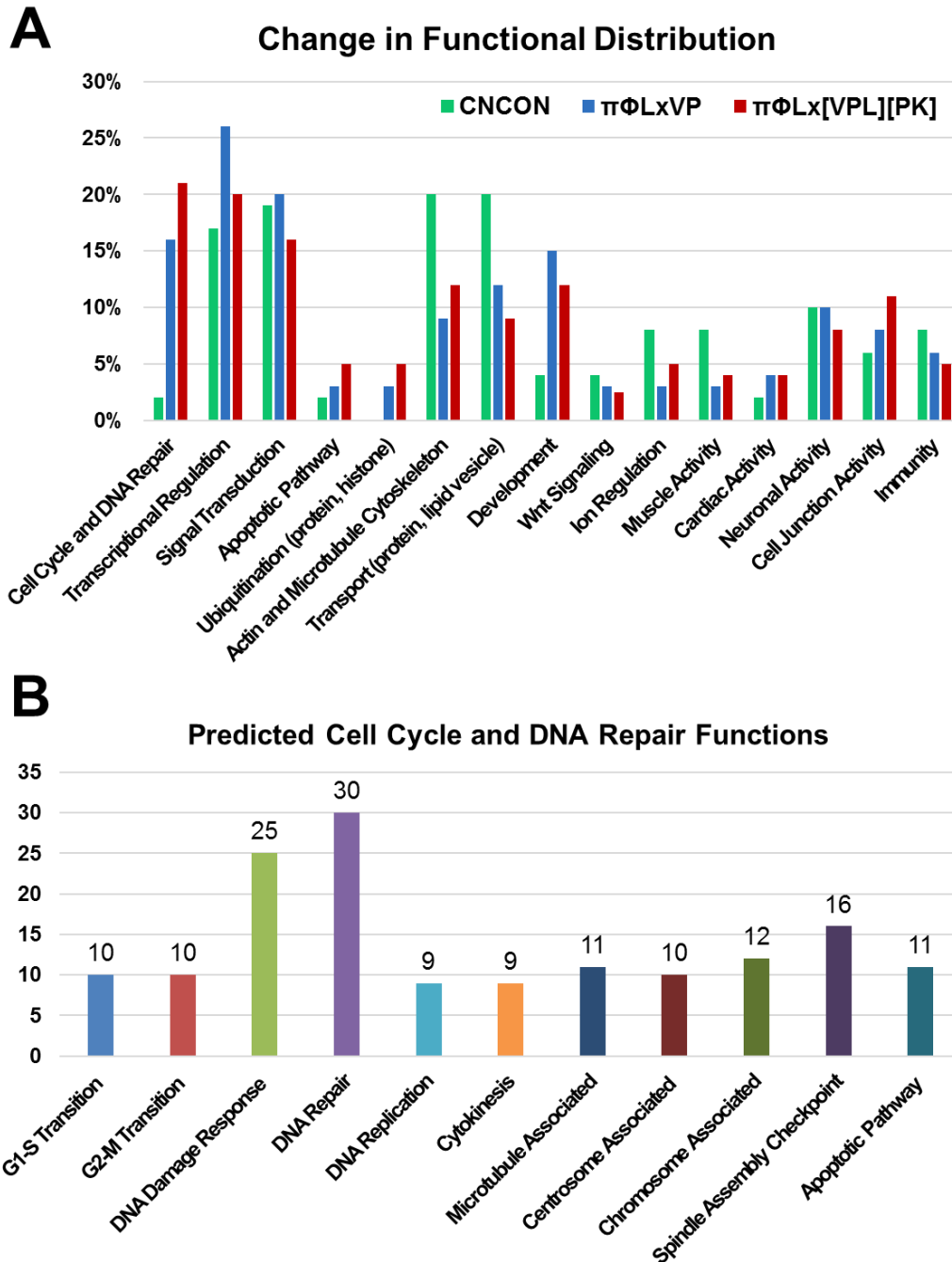
Figure S5.

A

Change in Functional Distribution

B

Predicted Cell Cycle and DNA Repair Functions

Figure S5. *Change in the functional distribution of CN activity among 3 databases.* **(A)** Comparison of the functional distribution of the proteins contained within CN[CON] (green), the π-ɸ-L-x-**V-P** database (blue) and the π-ɸ-L-x-**VPL-PK** database (red). **(B)** Distribution of the predicted CN interactors that have roles in cell cycle regulation and DNA repair.